UNCLASSIFIED

AAEC/E 59

AUSTRALIAN ATOMIC ENERGY COMMISSION

RESEARCH ESTABLISHMENT

LUCAS HEIGHTS

FAST NEUTRON FLUX AND SPECTRUM MEASUREMENTS IN HIFAR

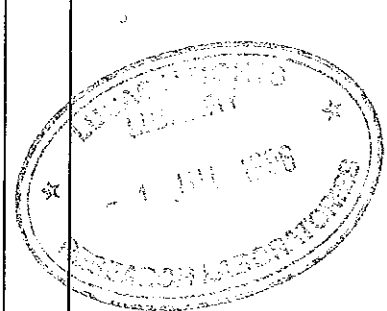

by

K. P. NICHOLSON

W. R. QUEALY

Issued Sydney, March 1961

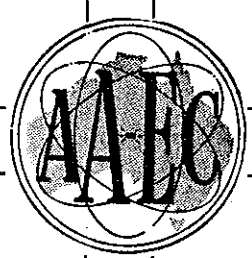

UNCLASSIFIED

AUSTRALIAN ATOMIC ENERGY COMMISSION

FAST NEUTRON FLUX AND SPECTRUM MEASUREMENTS IN HIFAR

by

K. P. NICHOLSON

W. R. QUEALY

Abstract

This report presents the results of measurements on the fast neutron fluxes and energy spectra in the core and 2V experimental facilities of HIFAR using threshold detectors. The following reactions were used: $P^{31}(n,p)Si^{31}$, $S^{32}(n,p)P^{32}$, $Ni^{58}(n,p)Co^{58}$, $Al^{27}(n,\alpha)Na^{24}$. The total fission flux in the flux scanning tubes was found to be 23 ± 3 per cent. of the total effective flux at the same position, having a maximum value of 4.3×10^{13} neutrons $cm^{-2}\,sec^{-1}$ (approximately 8.3 MW thermal), for a maximum effective flux of 1.7×10^{14} neutrons $cm^{-2}\,sec^{-1}$. A neutron energy spectrum differing only slightly from a fission spectrum shape was found in all positions. The use of the $Ni^{58}(n,p)Co^{58}$ reaction as a fast flux monitor is discussed.

CONTENTS

1. INTRODUCTION

Measurement of the neutron fluxes in the core and experimental facilities was one of the main parts of the A.A.E.C. Reactor Physics Section's calibration of HIFAR for the eleven, seventeen, twentyone and twentyfive element cores. The results are reported in McKenzie and Duncan (1958), Nicholson (1959) and Connolly and McKenzie (1960). In this work the neutron fluxes measured were referred directly to the reaction rate of a U^{235} fission counter which responds to neutrons over a wide range of energy. These fluxes correspond closely to the total "effective" flux (Westcott, 1956; Westcott et al., 1958; Hines and Symonds, 1958).

To calculate reaction rates in materials other than U^{235} it is necessary to know something about the energy spectrum of the neutrons in the reactor. A previous report (Quealy, 1959), outlined a programme of measurements to be made on the neutron spectrum in HIFAR and presented the results of some preliminary measurements in the epithermal region.

Separate experimental programmes using different methods are generally required for flux and energy spectrum measurements of neutrons depending on whether they are in the thermal, epithermal or fast neutron groups. Threshold detector measurements of the fast neutron fluxes and energy spectra in HIFAR are described in this report. Measurements of the epithermal spectrum have also been made and will be described in a separate report.

1.1 The Reactor Fast Neutron Spectrum

A very high proportion of the fast neutrons in HIFAR originate as fission neutrons. The small number of neutrons which originate from (γ, n) and (n, 2n) processes will not produce a significant change in the energy spectrum and may be neglected.

At high energies, say 6 MeV and above, the neutrons will be mostly unscattered fission neutrons so the energy spectrum will be very close to a pure fission spectrum. At lower energies the original fission energy spectrum will be modified by the addition of neutrons which have been scattered by the moderator. The spectrum of neutrons emitted in the fission of U^{235} has been measured experimentally by Cranberg et al.(1956) and is given by the following relation:

$$N(E) = 0.4527 \exp(-E/0.965) \sinh \sqrt{2.29E} \qquad (1)$$

The average energy of fission neutrons is 1.98 MeV. This fission spectrum will be used in the present measurements. Most of the other work referred to in this report makes use of the earlier fission spectrum of Watt (1948) which can be expressed as:

$$N(E) = 0.484 \exp(-E) \sinh \sqrt{2E}.$$

This spectrum is compared with that of Cranberg in Figure 1.

The energy at which the reactor spectrum departs significantly from a pure fission spectrum is discussed by Hogg and Weber (1960) for the MTR and ETR reactors. They conclude that the spectrum has a fission shape down to 1 MeV. In addition measurements by Trice (1958) in beams from several reactors did not show a significant departure from fission shape at the Np^{237} threshold (approximately 0.7 MeV) although there were wide variations in the thermal to fast flux ratio with position in the lattice.

Recent calculations (Rowlands, 1959, Pollard, 1960) also suggest that the spectrum should have a fission shape down to about 1 MeV. These calculations are referred to in greater detail in Section 4.

2. THE THRESHOLD METHOD OF DETECTING FAST NEUTRONS

Measurements of fast neutrons in the presence of high fluxes of thermal and slowing down neutrons as found in and near the core of a thermal reactor may be made using threshold reactions which are reactions induced only by neutrons of energy above a certain value called the threshold energy E_t. The ideal threshold detector would be based on a reaction which has zero cross section below its threshold energy and a constant value above this energy. The reaction rate in such a detector would measure the flux of neutrons having energies greater than E_t and by using a number of such detectors with different threshold energies it would be possible to determine the shape of the integral spectrum.

An ideal threshold reaction does not exist in practice but a number of reactions do approach it sufficiently well to be used for fast neutron spectrum measurements. These include the fission of Th^{232}, U^{238}, Np^{237} and some reactions in which a charged particle is emitted; e.g. (n,p) and (n, α) reactions. The cross section for these reactions rises from zero at E_t to a maximum value called the "saturation" cross section σ_{sat} after which it is more or less constant in the energy range of interest. The reason for this is that the probability of the reaction occurring is proportional to the probability of the charged particle penetrating the coulomb potential barrier and this increases with increasing energy of the neutron. When the barrier penetrability approaches unity the cross section approaches a maximum value.

An effective threshold energy E_{eff} can be defined for such a practical threshold detector by the following equation for a reaction rate R per atom:

$$R = \sigma_{sat} \int_{E_{eff}}^{\infty} \phi(E)dE = \int_{o}^{\infty} \sigma(E)\,\phi(E)dE = \bar{\sigma} \int_{o}^{\infty} \phi(E)dE \qquad (2)$$

where $\sigma(E)$ is the cross section as a function of E, $\bar{\sigma}$ is the average cross section per atom in a fission spectrum and $\phi(E)$ is the neutron flux as a function of E, assumed to be the fission neutron spectrum. The reaction can thus be regarded as an ideal threshold reaction having a cross section of zero for neutrons of energy below E_{eff}, and σ_{sat} for any energy above E_{eff}. The value of E_{eff} obviously depends on the actual neutron energy spectrum but for the detectors used it is not unduly sensitive to changes in the spectrum as the initial increase in the threshold cross section occurs over a small energy range. This is discussed in some detail by Trice et al. (1953).

As pointed out by Mellish et al. (1958), if $\phi(E)$ is assumed to be a fission spectrum then one actually measures an "effective" fission flux which is the undisturbed fission flux that would give the activity observed. Thus when the experimental results are compared with an integral fission spectrum, the existence of a fission shape for the reactor spectrum can either be confirmed or refuted. Any deviation would be a first approximation to a different spectral form, but to establish the form of the correct spectrum from the results direct reference to the excitation functions is necessary. In practice the experimental errors combined with the large energy intervals between the threshold energies of suitable detectors limit the extent to which the results can be analyzed for new spectra.

A generalized form of analysis which is not dependent on the assumption of a fast neutron energy spectrum has been developed recently by Trice (1957). The calculations use only the two fundamental parameters, namely the cross section as a function of neutron energy and the relative yields of each reaction in the unknown spectrum. This method of analysis was not used in this work.

The results are related to the new flux and cross section convention using the method of Roy and Wuschke (1959). The threshold reaction rate per atom R is defined in terms of the effective flux W and the effective cross section σ_F such that

$$R = \sigma_F W$$

$$= \sigma_F N v_o$$

where N is the total neutron density per cm^3 and v_o = 2200 m/s. Using the average cross section $\bar{\sigma}$ defined by equation 2 and the threshold reaction rate per atom R above, we have:

$$\sigma_F = \bar{\sigma} \frac{\int_o^\infty \phi(E)dE}{Nv_o} = \bar{\sigma} z \qquad (3)$$

where z is a fast neutron spectral index which will be a function of position in the reactor. In presenting the results, values of z are given along with the total effective fission fluxes.

From the experimental viewpoint the threshold method has a number of limitations. The cross section data for all but a few reactions of this type are limited, and not very accurately known. As outlined earlier in this section none of the excitation functions have the ideal threshold shape, the curve having a "tail" below the effective threshold energy. When used to detect neutrons with an energy distribution similar to a fission spectrum a significant fraction of the reaction rate given by equation 2 will be due to neutrons with energies below the effective threshold. These limitations complicate the interpretation of experimental results.

The fission detectors approximate closer to ideal threshold detectors, but suitable fission counters were not available at the time these measurements were made.

3. REACTIONS AND EXPERIMENTAL PROCEDURES USED

Four reactions were chosen for the fast neutron spectrum studies in HIFAR, the $P^{31}(n,p)Si^{31}$, $S^{32}(n,p)P^{32}$, $Ni^{58}(n,p)Co^{58}$ and $Al^{27}(n,\alpha)Na^{24}$ reactions. Details are summarized in Table 1.

TABLE 1

Threshold Reaction Data

Material Used	Reaction	Half Life	Counting Method
$NH_4H_2PO_4$ powder	$P^{31}(n,p)Si^{31}$	2.8 h	4π beta counting
NH_4HSO_4 powder	$S^{32}(n,p)P^{32}$	14.3 d	4π beta counting
Ni foil	$Ni^{58}(n,p)Co^{58}$	72 d	($\beta-\gamma$ coincidence ($\gamma-\gamma$ coincidence (γ analysis
Al foil	$Al^{27}(n,\alpha)Na^{24}$	15 h	$\beta-\gamma$ coincidence

The measurements were made on a core consisting of twentyfour Mark IIA fuel elements (box type each containing 100 g U^{235}) and one Mark III element (annular type containing 115 g U^{235}), which was either in the C3 or the E1 fuel element position. A plan view of HIFAR showing the vertical experimental facilities and fuel element positions is shown in Figure 2. Samples of all four detectors were irradiated in the Mark IIA fuel element flux scanning tubes and in a central ¾ inch diameter tube placed inside the Mark III fuel elements in the C3 and E1 positions. Sample positions of $-9\frac{1}{2}$, -2 and $+10$ inches were chosen to give values near the top and bottom of the core and at the position of maximum flux. The dimensions above give the distance in inches below (negative) and above (positive) the centre plane of the core. Additional measurements were made with $S^{32}(n,p)P^{32}$ and $Ni^{58}(n,p)Co^{58}$ reactions at the -2 inch position in C1, C2, D1, D3, 2V3, and 2V7 to measure the variation of fast flux over the core and just outside it. All irradiations were done at a maximum

effective flux of 1.95×10^{10} neutrons cm^{-2} sec^{-1} (0.92 KW thermal) the critical coarse control arm angle being 15.4^{o}.

All materials used were spectrographically analyzed to ensure that no troublesome impurities were present. The counting methods vary according to the detector used and are discussed under individual headings.

The conversion of reaction rate to neutron flux requires a knowledge of the reaction cross section as a function of energy. Then provided the spectrum under investigation does not differ a great deal from a fission spectrum shape and the saturation cross section σ_{sat} is known, it is possible to deduce a value for the effective threshold energy E_{eff}. An integral flux above E_{eff} can then be calculated. If only the cross section averaged over the fission spectrum $\bar{\sigma}$ is known, it is possible to measure only the total flux of fission neutrons, assuming the fast neutron spectrum has a fission spectrum shape.

An effort was made to evaluate the existing data and set up values to be adopted in this work. Values of $\bar{\sigma}$ and E_{eff} were computed using published data on the cross sections as a function of energy and are included in Table 2 along with much of the experimental data (a useful summary is given by Rochlin, 1959). Most of the published cross sections are $\bar{\sigma}$ values measured relative to the $S^{32}(n,p)P^{32}$ or the $Al^{27}(n,\alpha)Na^{24}$ reactions.

TABLE 2

Cross Section Data

Reaction	Data by	$\bar{\sigma}$, measured, mb	$\bar{\sigma}$, calculated	E_{eff}, MeV	σ_{sat}, mb
$P^{31}(n,p)Si^{31}$	Hughes et al., 1949	19		3.5	
	Richmond and Phillips, 1957	31.2			
	Passell and Heath, 1960		30	2.9	
	Trice, 1955		22.8	2.4	75 Hughes et al., 1949
	This report		30	3.0	142 Grundl et al., 1958
$S^{32}(n,p)P^{32}$	Hughes et al., 1949	30		3.5	
	Passell and Heath, 1960		65	3.0	
	Richmond and Phillips, 1957	60.3			
	Trice, 1955	63		2.8	280 Hughes et al., 1949
	This report		62	3.2	340 Allen et al., 1957
$Ni^{58}(n,p)Co^{58}$	Hughes et al., 1949			4.1	
	Passell and Heath, 1960	91			
	Trice, 1955	66.4		5.0	1230
	Rochlin, 1959	140			
	Mellish, Payne and Otlet, 1958	45*			
	Schuman and Mewherter, (see Rochlin, 1959)				
	Robinson and Fink (see Rochlin, 1959)	225			
$Al^{27}(n,\alpha)Na^{24}$	Hughes et al., 1949	0.6		8.7	
	Richmond and Phillips, 1957	0.6			
	Passell and Heath, 1960		0.59	8.15	
	Trice, 1955			8.1	111 Trice, 1955
	This report		0.54 ±0.07		116 Grundl et al., 1958

* Relative to 30 mb for $S^{32}(n,p)P^{32}$

A discussion of the cross sections to be adopted and their interpretation in the measurement of fast neutron spectra is given by Trice (1955). His figures are based on yield curves weighted by the fast neutron spectrum which is assumed to be a pure fission spectrum at high energies.

3.1 The $P^{31}(n,p)Si^{31}$ Reaction

Phosphorus was irradiated in the form of powdered ammonium dihydrogen phosphate ($NH_4H_2PO_4.6H_2O$). Samples of this compound were prepared by packing about 20 mg into a ¾ inch length of polythene tubing of 2 mm inside diameter and 0.6 mm wall thickness. The tube was sealed by fusing the ends in a jet of hot air. Each sample was placed in a cylindrical cadmium box of 0.040 inch wall thickness to eliminate thermal neutrons which could cause the build up of undesirable activities (e.g. P^{32}). Irradiation times of one hour gave activities of 10^3 to 10^4 disintegrations per minute per milligram (dpm/mg).

During this irradiation P^{32} was also produced by radiative capture of epithermal neutrons. However, the P^{32} activity at the time the sample was removed from the reactor was an order of magnitude less than the S^{31} activity, so that chemical separation was not necessary. The activities were determined by absolute beta counting with a 4π flow type proportional counter.

The cross section data used were based on the results of Grundl et al. (1958) which are shown in Figure 4. Using this curve and assuming the spectrum to be that of Cranberg et al. (1956), new values of E_{eff} and $\bar{\sigma}$ were calculated from equation 2. The calculated average cross section of 30 mb differs significantly from the early measurements of Hughes et al. (1949) and the calculations of Trice (1955) but is in good agreement with the result of Richmond and Phillips (1957).

3.2 The $S^{32}(n,p)P^{32}$ Reaction

Sulphur was irradiated as ammonium bisulphate (NH_4HSO_4) powder. The P^{32} activity decays by beta emission only and has a half life of 14.3 days. The samples were prepared, irradiated and counted in exactly the same way as the $P^{31}(n,p)Si^{31}$ samples. Irradiation times of about three hours gave activities of a few hundred disintegrations per minute per milligram. No other activities were detected when the counting was started two days after the irradiation.

Values of the cross section are listed in Table 2 along with the value calculated using the excitation function of Allen et al. (1957) and shown in Figure 4. This result gives additional evidence for a $\bar{\sigma}$ in the region of 60 mb, our value being 62 mb.

3.3 The $Al^{27}(n,\alpha)Na^{24}$ Reaction

Foils of aluminium the same size and thickness as the nickel foils, each weighing about 4 mg were irradiated under cadmium for 5½ hours. Activities of 1000 to 4000 disintegrations per minute were obtained. In addition to Na^{24} which has a 15 hour half-life, Al^{28} and Mg^{27} from the (n,γ) and (n,p) reactions, which have half lives of 2.3 and 9.5 minutes respectively, are formed. The foils were left overnight to allow the Al^{28} and Mg^{27} to decay, and were then compared using G-M counters. The most active of the foils in each batch was counted absolutely by the beta-gamma coincidence method.

A check was made on the value of $\bar{\sigma}$ for this reaction using the cross section data of Grundl et al. (1958). The measurements cover the energy range 6.7 to 9.0 MeV (see Figure 4) with an additional value of 116 ±8 mb at 14.1 MeV. An extrapolation was made between 9 and 14 MeV, an estimate of the error introduced by this extrapolation being included in the error in $\bar{\sigma}$. The value obtained was (0.54 ± 0.07) barn. It is clear from the shape of the cross section curve that there is no evidence of a saturation value at neutron energies less than 14 MeV. Therefore the parameters E_{eff} and σ_{sat} used in the integral spectrum analysis will be difficult to define. For an approximate examination of the integral flux data we used E_{eff} = 8.1 MeV and σ_{sat} = 116 mb. It can be shown however, using the cross sections of Grundl et al. (1958) and the fission spectrum of Cranberg (1956) that the reaction rate can be characterized by an E_{eff} of 7.5 MeV and σ_{sat} of 65 mb with equal validity.

3.4 The $Ni^{58}(n,p)Co^{58}$ Reaction

The nickel metal foils used were 0.001 inch thick and 3/16 x 5/8 inches in area, each foil weighing approximately 20 mg. They were irradiated for 5½ hours and gave activities of about 300 dpm/mg. The decay scheme of Co^{58} and Co^{58m} (Strominger et al., 1958) is shown in Figure 3 to assist in explaining the following counting procedures.

Other reactions which occur in the Ni foil are $Ni^{62}(n,\gamma)Ni^{63}$ (half life 80 years), $Ni^{64}(n,\gamma)Ni^{65}$ (half life 2.6 hours) and $Ni^{60}(n,p)Co^{60}$ (half life 5.3 years).

Before counting, the foils were left for ten days to allow the Co^{58m} and the shorter activities to decay. Gamma spectrum analysis showed that all other activities could be neglected. The relative activities of the foils were measured with a high geometry G–M counter and the absolute activity of the two most active foils in each series of measurements was determined by beta–gamma coincidence counting.

Care must be taken in this measurement to avoid spurious coincidences from annihilation gamma rays and Compton scattered gammas. The former were eliminated by placing the beta and gamma scintillators at 90° with respect to the source. Compton coincidences were reduced to less than the statistical errors of the results by mounting a wedge–shaped lead shield on a line bisecting the angle between the detectors.

The beta–gamma coincidence technique used was checked by comparing the absolute activity of a more active foil with the result obtained by the gamma–gamma coincidence method, which in turn was checked using a standard Co^{60} source. In these measurements the nickel foil was wrapped in sufficient aluminium to absorb the positions completely and coincidences between the annihilation photons and the 0.8 MeV gammas were observed. As with the beta–gamma method, the detectors (in this case two identical NaI(Tl) crystals) were placed at 90° to avoid spurious coincidences from the annihilation photons and a wedge–shaped lead shield used to reduce the Compton coincidence rate. The result for the beta–gamma and gamma–gamma methods agreed to within ± 5 per cent. As a further check the same nickel foil was gamma counted using the 0.8 MeV gamma. The coincidence results were confirmed within the experimental error, ± 8 per cent.

The Co^{58} activities of the irradiated nickel foils and the high activity foil were also checked by absolute beta counting and some anomalous results obtained. The beta activities were at least 50 per cent. higher than the coincidence figures. It is thought that this discrepancy is due to absorption of the K x–rays from Fe^{58} associated with 86 per cent. of the Co^{58} disintegrations. A similar correction, for Cu^{64} decay, is mentioned by Pularikas and Fink (1959) who adopt a counting efficiency of 10 per cent. for the K x–rays of Ni^{64}. It is hoped that further experiments will explain this discrepancy. The results used in this report are those obtained by the coincidence method and gamma counting.

No detailed excitation function has been measured for the $Ni^{58}(n,p)Co^{58}$ reaction, so the theoretical barrier penetrability (Bethe, 1937) is used together with the value of σ_{sat} of 1230 mb given by Trice (1955). The $\bar{\sigma}$ and E_{eff} he obtained are 66.4 mb and 5.0 MeV respectively. Also available are the recent results of Passel and Heath (1960) who use $\bar{\sigma}$ of 91 mb and E_{eff} (after Hughes, 1953) of 4.1 MeV. The results of Passel and Heath are in good agreement with those of Mellish et al. (1958). Despite the agreement of the latter two, it is apparent from the summary of Rochlin (1959) that a considerable discrepancy exists in the values of $\bar{\sigma}$. It is of interest to consider the values of $\bar{\sigma}$, obtained by Trice (1955) for a series of positions in the MTR. Cross sections ($\bar{\sigma}$) from 66.4 mb down to 35.1 mb were observed with increasing distances from the core. The form of the excitation function is most likely to explain this behaviour. If it varies greatly from the ideal threshold reaction shape and increases relatively slowly over the energy range of interest for fission neutrons, then $\bar{\sigma}$ and E_{eff} will become sensitive to small changes in the neutron energy spectrum.

For an initial examination of the Ni^{58} results, we used a σ_{sat} of 1230 mb and E_{eff} of 5.0 MeV taken from Trice (1955). It is clear that in the absence of detailed cross section data the $Ni^{58}(n,p)$ reaction cannot be used as a reliable fast flux monitor in irradiation experiments.

4. RESULTS AND DISCUSSION

4.1 Fast Neutron Spectrum and Absolute Fluxes in the Core of HIFAR

The threshold method gives directly integral fast flux values above the effective threshold energy provided the spectrum does not differ greatly from a fission spectrum shape. These results are shown in Table 3 for each of the four detectors used at three positions in the C3 and E1 fuel element positions.

TABLE 3

Integral fast flux above threshold at maximum effective flux of 1.7×10^{14} neutrons cm^{-2} sec^{-1}. Fluxes in units of 10^{12} neutrons cm^{-2} sec^{-1}.

Position	3.0 MeV (P^{31})	3.2 MeV (S^{32})	5.0 MeV (Ni^{58})	8.1 MeV (Al^{27})	Total fission
(a) Mark IIA element in C3, Mk. III hollow element in E1.					
C3/-9½	7.8	5.3	1.25	0.20	33
C3/-2	9.5	6.3	1.45	0.27	40
C3/+10	4.8	2.9	0.65	0.13	18
E1/-9½	5.7	4.0	0.86	0.13	23
E1/-2	6.9	4.6	0.99	0.15	27
E1/+10	3.0	1.7	0.41	0.065	11
(b) Mark III hollow element in C3, Mk. IIA element in E1.					
C3/-9½	8.8	7.4	1.45	0.23	41
C3/-2	9.4	8.6	1.72	0.30	46
C3/+10	5.4	3.8	0.86	0.14	23
E1/-9½	4.8	3.8	0.66	0.12	21
E1/-2	5.0	4.4	0.99	0.16	24
E1/+10	2.2	1.7	0.37	0.069	10

Measurements were taken in the flux scanning tubes of the normal MkIIA fuel elements and in a flux scanning tube fitted in the centre of a Mk III fuel element. The annular space between the flux tube and the Mk III fuel element was filled with D_2O.

The effective total fission fluxes given in the right hand column of Table 3 were obtained by fitting an integral fission spectrum to the experimental values in the table, and are therefore based on the assumption that the fast neutron spectrum is a fission spectrum below 3 MeV as well as above it.

The results of all the spectrum measurements are consistent, within the experimental error, with a fast neutron spectrum having approximately the same shape as the fission spectrum over the energy range covered by the detectors used. This is illustrated in Figure 5 for a few typical points. The values of the integrated flux measured by the $Al^{27}(n, \alpha)$ reaction always lie above the fission spectrum fitted to the fluxes from the P^{31} and S^{32} reactions. The evidence is sufficient to indicate a small deviation from the fission spectrum shape between the S^{32} and the Al^{27} thresholds.

The total fission flux values given in Table 3 were calculated by extrapolating the best fit integral fission spectrum to zero energy. These extrapolated values are compared in Table 4 with the total effective fission fluxes calculated using the preferred values of $\bar{\sigma}$ for the P^{31}, S^{32} and Al^{27} detectors. The differences in the total effective fission fluxes measured by the P^{31} and S^{32} reaction at lower energies and the Al^{27} reaction at high energy provide additional evidence of a deviation of the reactor spectrum from the fission spectrum shape.

TABLE 4

Total effective fission flux values for maximum effective flux of 1.7×10^{14} n cm^{-2} sec^{-1} using average cross sections and observed average cross sections for Ni^{58}. Fluxes in units of 10^{13} neutrons cm^{-2} sec^{-1}.

Element Type	Position (inches)	P^{31} $\bar{\sigma}$ = 30 mb	S^{32} $\bar{\sigma}$ = 60 mb	Al^{27} $\bar{\sigma}$ = 0.60 mb	Total effective fluxes from Table 3	$\bar{\sigma}$ for Ni^{58} based on Table 3 fluxes (mb)
Mk II, 100 g	C3/ -9½	3.7	3.0	3.8	3.3	44
	-2	4.5	3.5	5.1	4.0	41
	+10	2.3	1.7	2.4	1.8	40
Mk III, Hollow Element	C3/ -9½	4.2	4.1	4.5	4.1	43
	-2	4.4	4.9	5.7	4.6	45
	+10	2.6	2.2	2.7	2.3	46
Mk II 100 g	E1/ -9½	2.3	2.2	2.3	2.2	37
	-2	2.4	2.5	3.0	2.4	51
	+10	1.0	0.97	1.3	1.0	45
Mk III Hollow Element	E1/-9½	2.7	2.3	2.5	2.3	42
	-2	3.3	2.6	3.0	2.7	41
	+10	1.4	0.95	1.3	1.1	43

An indication of the reactor flux spectrum to be expected is given by the slowing down spectra in D_2O calculated by Rowlands (1959) and Pollard (1960) for a uniformly distributed source of fission neutrons. The flux per unit lethargy of Pollard for D_2O (zero buckling) is shown in Figure 6 together with a fission spectrum normalized to a mean value at 2.0 MeV. It appears that in this special case the spectrum above 1 MeV has very nearly the shape of a fission spectrum though only a fraction of the flux (46 per cent. at 3.0 MeV) consists of unscattered fission neutrons.

Our results cannot be compared directly with the above calculations as in a heterogeneous reactor the spectrum is expected to vary widely between different positions in a lattice cell. In this work most measurements were taken on the outside surface of the box type (Mk II) fuel elements so that the contribution to the total fast flux from unscattered fission neutrons would be somewhat greater than in a homogeneous system. Conversely, at positions in the lattice removed from the fuel elements, the spectrum of unscattered fission neutrons would be distorted as a result of the variation with energy of the D_2O cross section. This latter situation also applies to the 2V experimental holes of HIFAR. However the ratio of moderator to fissile material is high for this reactor, also the fuel is distributed over a comparatively large volume, thus a marked deviation from the slowing down spectrum of Pollard is unlikely, with the error becoming less as the energy increases.

The slowing down flux spectrum in Figure 6 shows a number of fluctuations due to variations in the D_2O scattering cross section. The dip in the energy range 3 MeV to 4 MeV is particularly important. It makes the average slope of the integral flux curve less than that of the integral fission curve above the S^{32} threshold in qualitative agreement with the observed integral flux spectra.

Weighted yield curves (i.e. reaction rate as a function of neutron energy) for the $S^{32}(n,p)P^{32}$ reaction using the slowing down spectrum of Pollard and the normalized fission spectrum given in Figure 6 show that the ratio

$$\frac{\text{Reaction rate } S^{32} \text{ in } D_2O \text{ spectrum}}{\text{Reaction rate } S^{32} \text{ in normalized fission spectrum}} = 0.87 .$$

This spectrum deviation could be the cause of the experimentally observed ratio

$$\frac{\text{Flux from the } S^{32}(n,p)P^{32} \text{ reaction}}{\text{Flux from the } A^{27}(n,\alpha)\,Na^{24} \text{ reaction}} = 0.84 \pm 0.06 .$$

The total effective fission fluxes of Table 3 are used to derive values of $\bar{\sigma}$ for the $Ni^{58}(n,p)Co^{58}$ reaction. The cross section ranges from 37 mb to 51 mb with a mean value of (43.1 ± 3.4) mb. This value is low compared with several other measurements (see Table 2) and may possibly be due to the different energy spectrum in the D_2O compared with the spectrum in the MTR Be reflector (Trice, 1955; Passell and Heath, 1960) and that in a natural uranium cartridge (Mellish et al. 1958).

As indicated above this difference can arise when the excitation function deviates considerably from that of the ideal threshold detector. This is probably the case for the Ni^{58} reaction. Preliminary investigations into the shape of the $Ni^{58}(n,p)Co^{58}$ excitation function indicate a slow increase of yield with energy, with a much higher cross section below 5.0 MeV (the E_{eff} assumed in section 3.4) than is indicated by the proton penetrability for Ni. These differences also cast doubt on the σ_{sat} of 1230 mb. Moreover since it appears that the shape of the excitation function departs greatly from that of the ideal threshold detector, such values as E_{eff} and σ_{sat} are difficult to define.

4.2 Relative Fast Fluxes and Flux Distribution

Relative fast flux values at a number of representative points in and just outside the core are given in Table 5, together with the value of z defined by equation 3. The variation of fast flux with radial distance from the core centre is shown in Figure 7.

TABLE 5

Relative Fast Fluxes and Values of the Spectral Index z

Position	Element Type	Detector	Relative fast flux	z	Distance from core centre (cm)
C3/-2	HFE	S Ni	1.39 1.15	0.30 0.27	0
C3/-2	100 g	S Ni	1.00 1.00	0.21 0.22	3.8
C2/-2	100 g	S Ni	1.00 0.975	0.21 0.22	11.4
D3/-2	100 g	S	0.93	0.20	15.8
C1/-2	100 g	S Ni	0.78 0.925	0.21 0.28	27.3
E1/-2	100 g	S Ni	0.71 0.60	0.26 0.24	36.0
E1/-2	HFE	S Ni	0.74 0.675	0.26 0.26	38.1
D1/-2	100 g	Ni	0.60	0.23	37.6
2V3/-2	100 g	S Ni	0.09 0.125	0.03 0.04	45.7
2V7/-2	100 g	Ni	0.075	0.03	55.4

The fast flux variation over the core gradually decreases with distance from the centre of the core to the edge, and rapidly decreases outside it. The ratio z in the fuel element flux scanning tubes varies only slightly with the position of the fuel element, as would be expected since the production of fission neutrons at a point in a fuel element is proportional to the thermal flux at that point. The fast flux in a hollow fuel element is approximately 20 per cent. higher than in a flux scanning tube of a Mk II (box type) fuel element in the same position for inner positions of the core. For the outside fuel elements, e.g. E1, the relative values will be dependent on the orientation of the flux scanning tube because of the rapid decrease of the fast flux in this region.

The total effective flux at C3/-2 was measured by a gold foil irradiation, and the total effective flux values at the other positions are based on the relative effective fluxes given by Connolly and McKenzie (1960). These measurements were made under slightly different core conditions from the fast neutron measurements (coarse control arm angle 18°), so the fast-effective ratios at these other positions are only approximate. The difference in values of fast flux between the top and bottom of the core is probably due to the thermal flux depression caused by the coarse control arms.

4.3 Accuracy of Results

The results are subject to two main sources of error, inaccuracies in the nuclear data used, including assumptions concerning the reactor flux spectrum, and experimental errors. In all cases the nuclear data are less reliable than the counting techniques.

The values of σ_{sat} for $P^{31}(n,p)Si^{31}$ and $S^{32}(n,p)P^{32}$ have an error of ± 10 per cent. As pointed out in Sections 3.3 and 3.4 the parameter σ_{sat} is difficult to define for the $Al^{27}(n,\alpha)Na^{24}$ and the $Ni^{58}(n,p)Co^{58}$ reactions so that the error on the figures quoted in Table 2 is probably 20 per cent. or more.

Values of E_{eff} also have errors of ± 10 per cent. except for Ni^{58} which is probably higher. The relative counting errors vary between ± 5 per cent. for aluminium and nickel and ± 8 per cent. for phosphorous and sulphur. The absolute counting errors are ± 10 per cent. or better. Thus the relative fluxes are accurate to ± 8 per cent. or better and the absolute total fluxes have errors of approximately ± 15 per cent.

5. ACKNOWLEDGMENTS

The authors gratefully acknowledge many helpful discussions with Dr. J.L.Symonds, the co-operation of the Analytical Chemistry Group who did all the absolute beta counting and the assistance of the Reactor Operations Group during the irradiations.

6. REFERENCES

Allen, L. Jr., Biggers, W.A., Prestwood, R.J. and Smith, R.K. (1957). Cross Sections for the $S^{32}(n,p)P^{32}$ and $S^{34}(n,\alpha)Si^{31}$ reactions. Phys. Rev. 107: 1363.

Bethe, H.A. (1937). Nuclear Physics. B. Nuclear dynamics, theoretical. Rev. Mod. Phys. 9, 69: see p. 163.

Connolly, J.W. and McKenzie, C.D. (1960). Reactor physics studies on the HIFAR twenty five element cores. AAEC/TM64.

Cranberg, L., Frye, G., Nereson, N. and Rosen, L. (1956). Fission neutron spectrum of U235. Phys. Rev. 103 : 662.

Grundl, J.A., Henkel, R.L. and Perkins, B.L. (1958). $P^{31}(n,p)Si^{31}$ and $Al^{27}(n,\alpha)Na^{24}$ cross sections. Phys. Rev. 109 : 425.

Hines, K.C. and Symonds, J.L. (1958). A flux and cross section convention. AAEC Internal Report K295.

Hogg, C.H. and Weber, L.D. (1960). E.T.R. fast neutron flux measurements. HDO-16535 USAEC report.

Hughes, D.J., Spatz, W.D.B. and Goldstein, N. (1949). Capture cross sections for fast neutrons. Phys. Rev. 75 : 1781.

Hughes, D.J. (1953). Pile Neutron Research. Addison Wesley Publishing Co., Cambridge, Mass.

McKenzie, C.D. and Duncan, M.E. (1958). Reactor physics studies on the HIFAR eleven element core. AAEC Internal report K242.

Mellish, C.E., Payne, J.A. and Otlet, R.L. (1958). Flux and cross section measurements with fast neutrons in BEPO and DIDO. AERE I/R 2630.

Nicholson, K.P. (1959). Reactor physics studies on the HIFAR seventeen and twenty one element cores. AAEC Internal report K266.

Passell, T.O. and Heath, R.L. (1960). Fission neutron cross section measurements for threshold reactions: nickel as a useful fast flux monitor. To be published.

Pollard, J.P. (1960). Spectrum calculations for neutrons slowing down by elastic collisions. AAEC/E54.

Poularikas, A. and Fink, R.W. (1959). Phys. Rev. 115: 989.

Quealy, W.R. (1959). Neutron flux and energy spectrum measurements in HIFAR. AAEC Internal report K306.

Richmond, R. and Phillips, J.A. – unpublished, see Phillips, J.A. (1957). The (n,2n) cross section of Th^{232} for fission neutrons. AERE report R/R 2366.

Rochlin, R.S. (1959). Fission neutron cross sections for threshold reactions. Nucleonics 17, No. 1: 54.

Rowlands, G. (1959). Numerical study of the fast neutron spectrum in homogeneous media. AERE report R3160.

Roy, J.C. and Wuschke, D. (1959). Fast neutron reactions and fast neutron flux in the NRX reactor. AECL 877.

Strominger, D., Hollander, J.M. and Seaborg, G.T. (1958). Table of isotopes. Rev. Mod. Phys. 30: 585.

Trice, J.B., Muckenthaler, F.J., Smith, F.W. and Johnson, E.B. (1953). Two neutron energy measurements in the bulk shielding facility using radioactivants. USAEC report AECD-3716.

Trice, J.B. (1955). A series of thermal, epithermal and fast neutron measurements in the MTR. USAEC report CF-55-10-140.

Trice, J.B. (1957). Preliminary report of an analytical method for measuring neutron spectra. USAEC report APEX 408.

Trice, J.B. (1958). Measuring reactor spectra with thresholds and resonances. Nucleonics 16, No. 7: 81.

Watt, B.E. (1948). Energy spectrum of neutrons from fission induced by thermal neutrons. USAEC report LA-718.

Westcott, C.H. (1956). The specification of neutron flux and effective cross sections in reactor calculations. AECL 352.

Westcott, C.H., Walker, W.H. and Alexander, T.K. (1958). Effective cross sections and cadmium ratios for the neutron spectra of thermal reactors. Geneva conference paper 15/P/202.

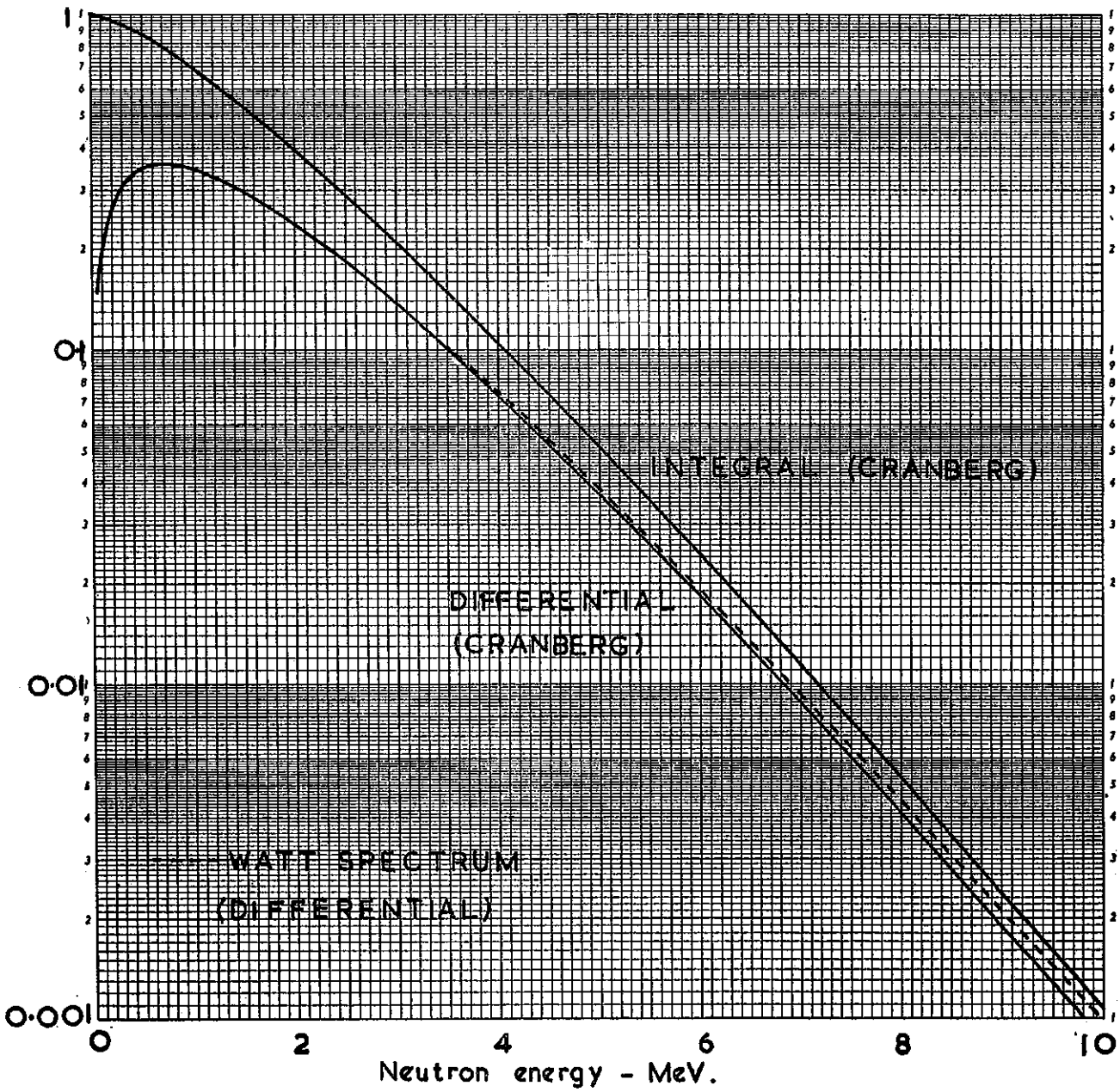

FIGURE I. THE FISSION SPECTRUM FOR U^{235}
(for unit source strength)

ARCUS No. 91

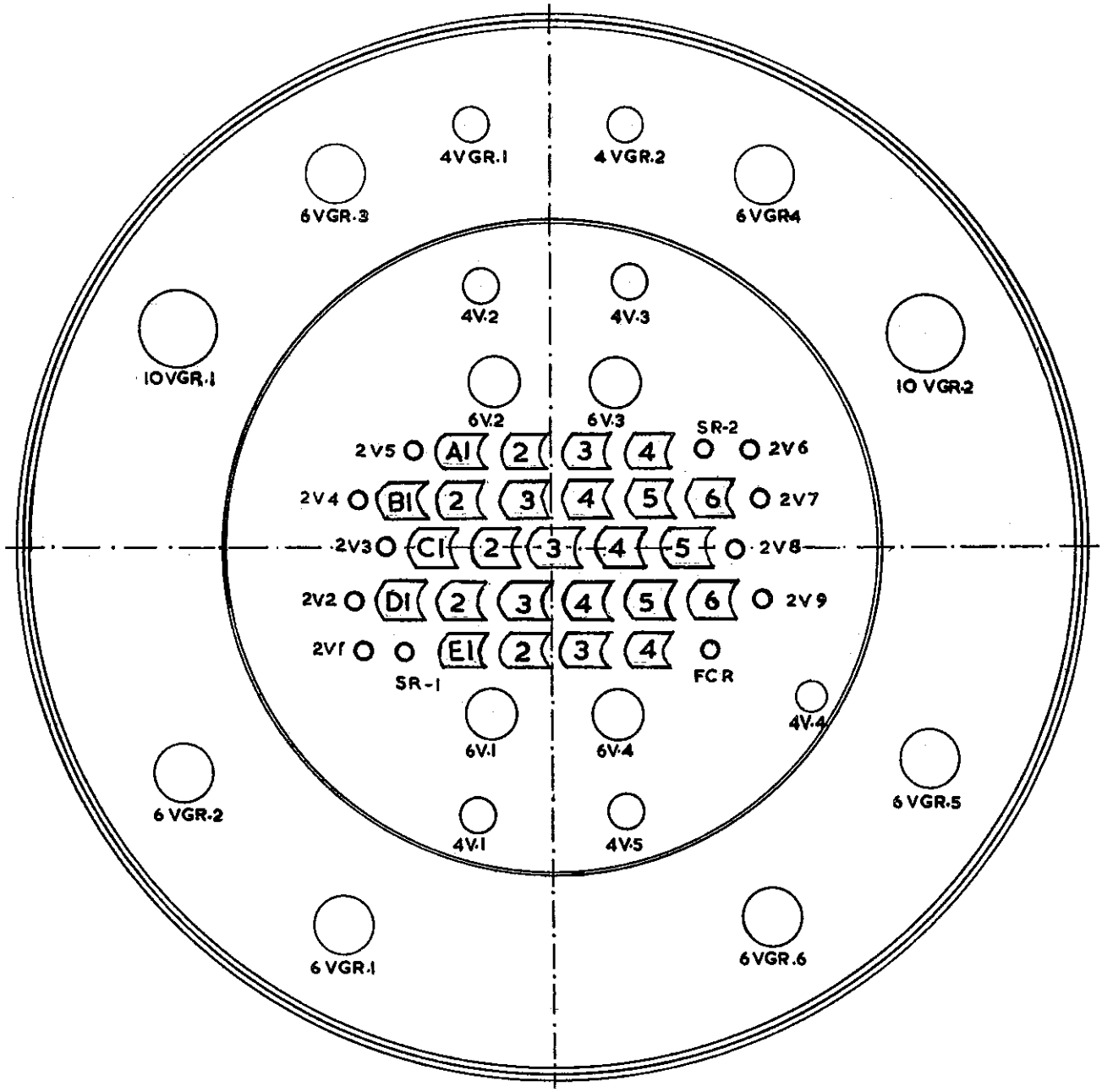

FIGURE . 2. PLAN VIEW OF HIFAR

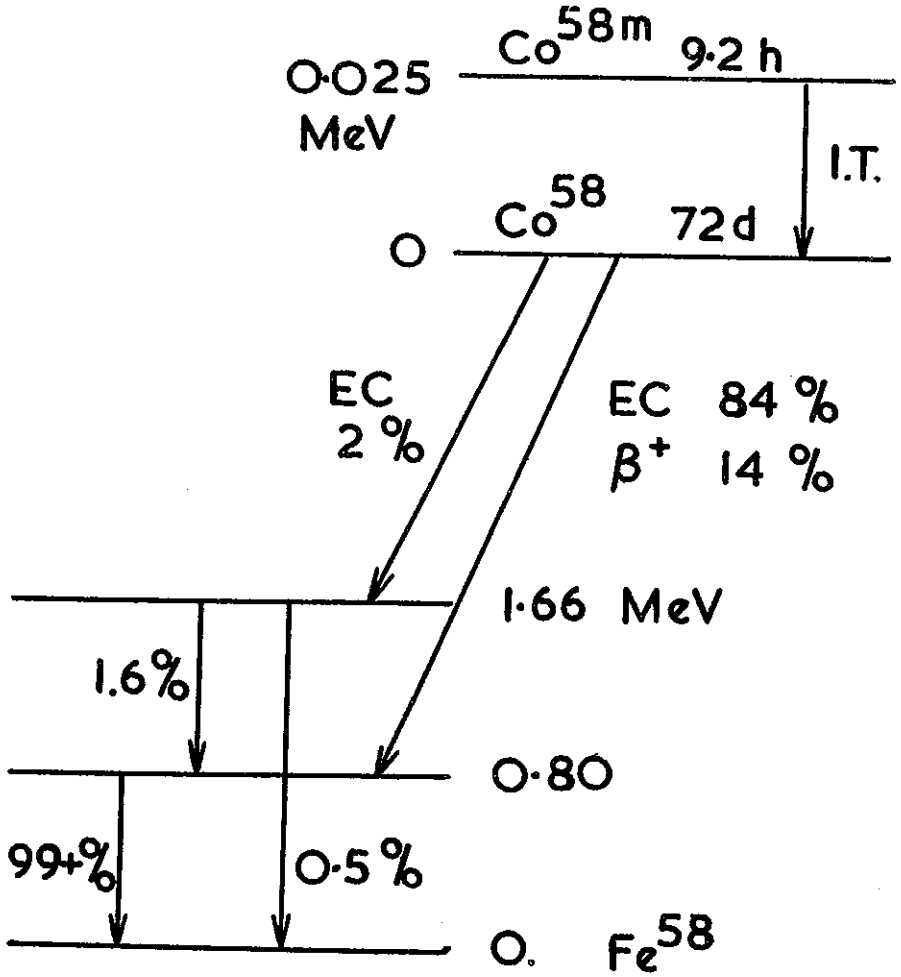

FIGURE 3 DECAY SCHEME OF Co^{58}

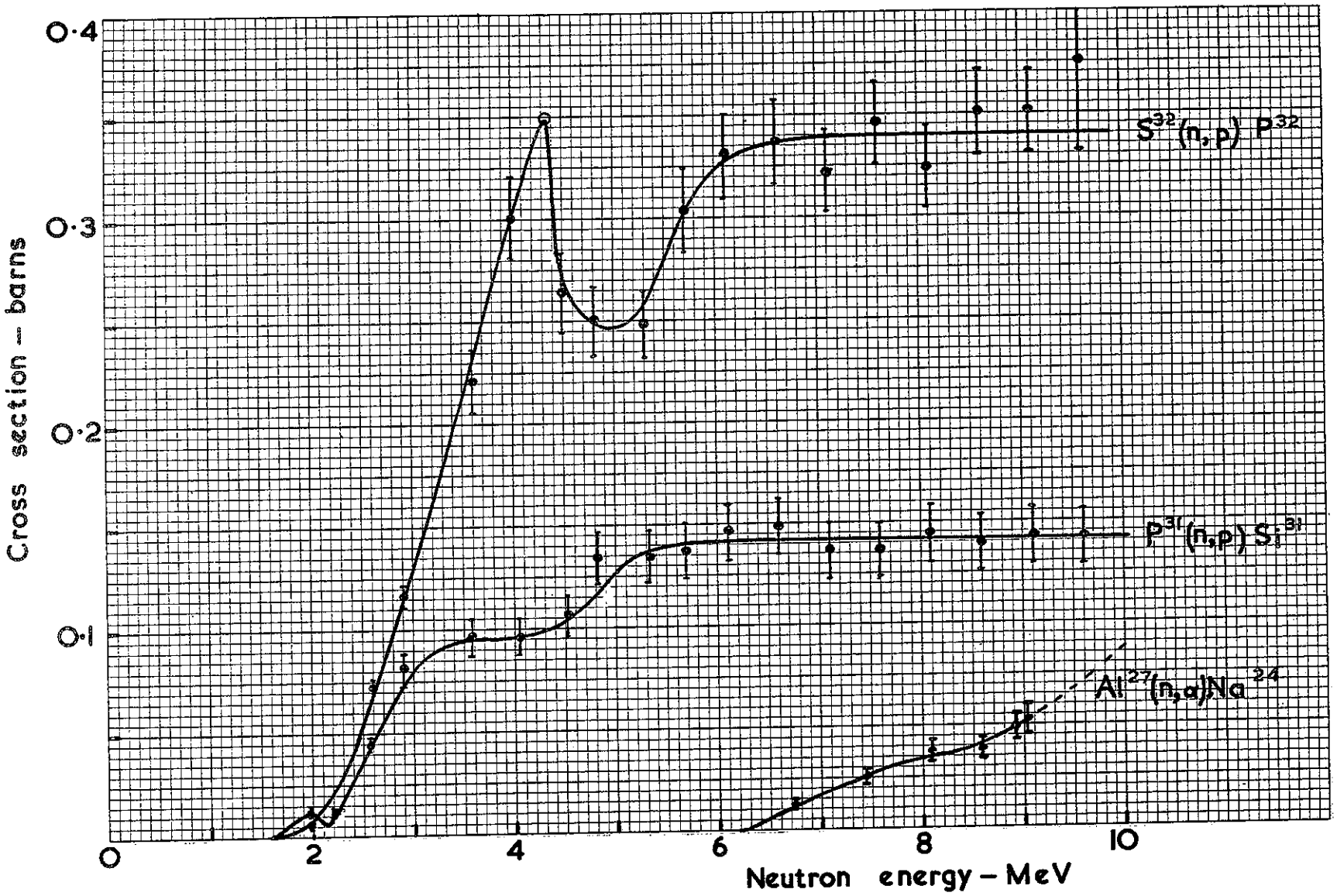

FIGURE 4 THRESHOLD REACTION CROSS SECTIONS

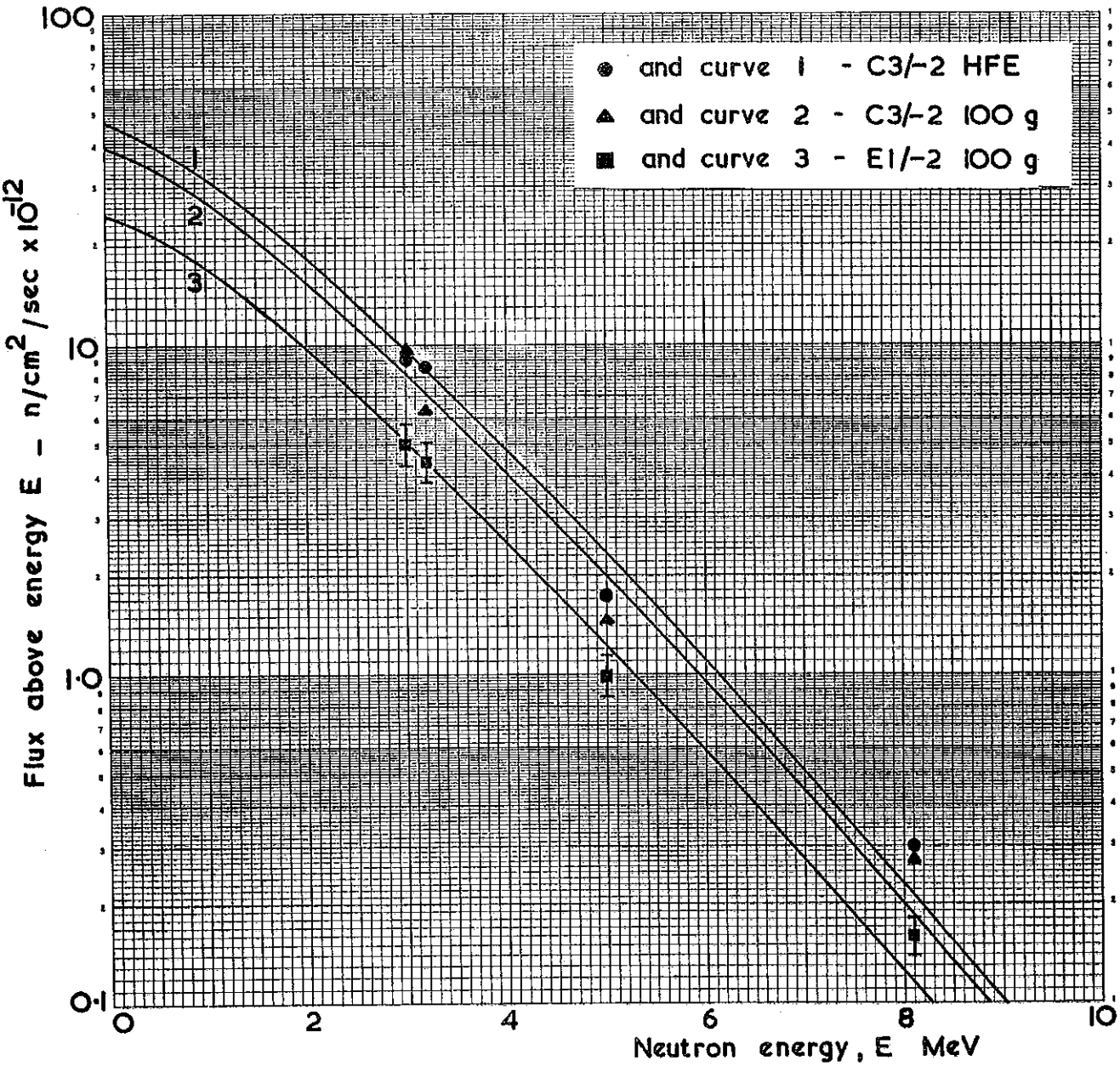

FIGURE 5 INTEGRAL FAST NEUTRON SPECTRA

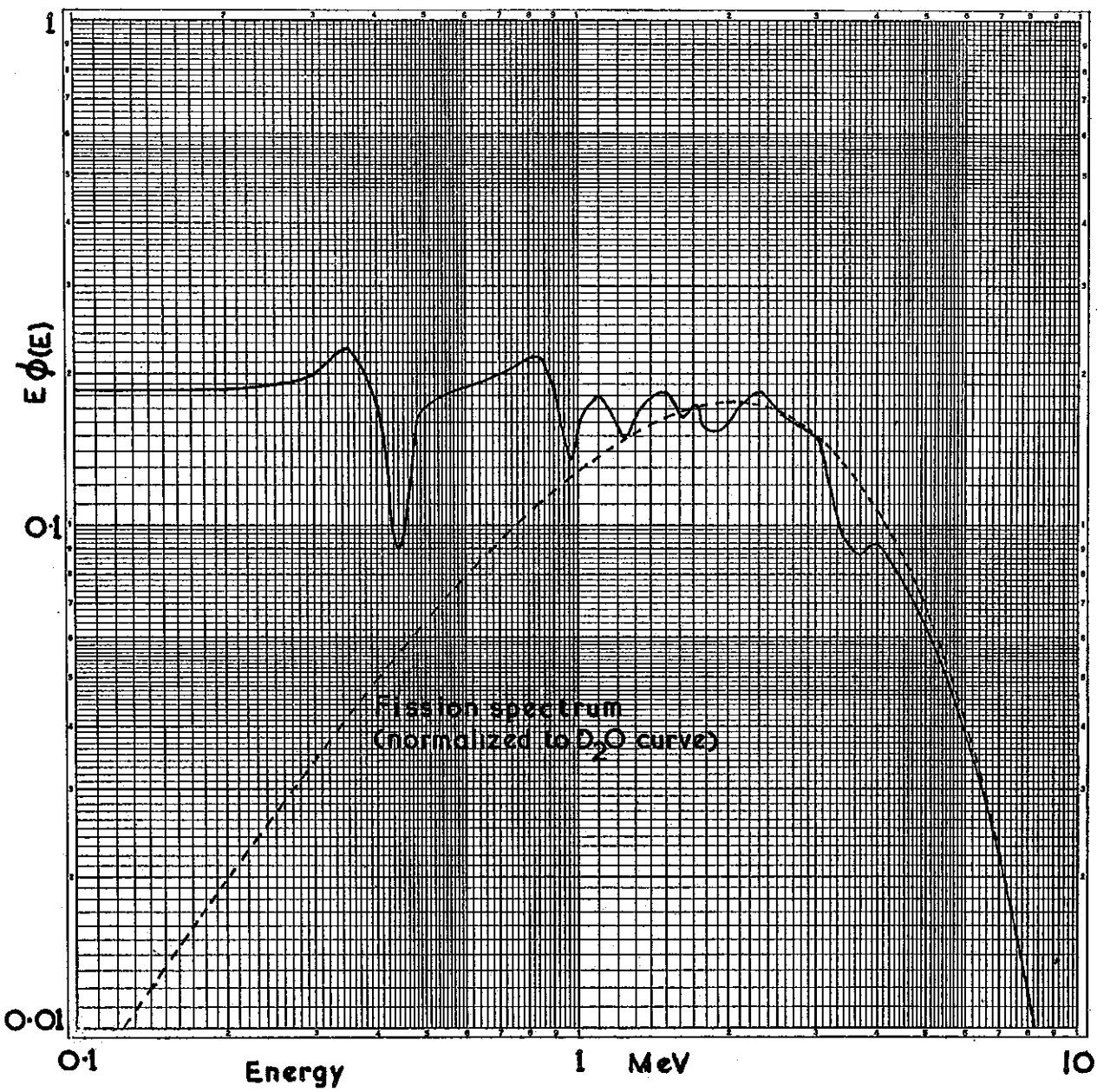

FIGURE 6 CALCULATED SPECTRUM IN D_2O

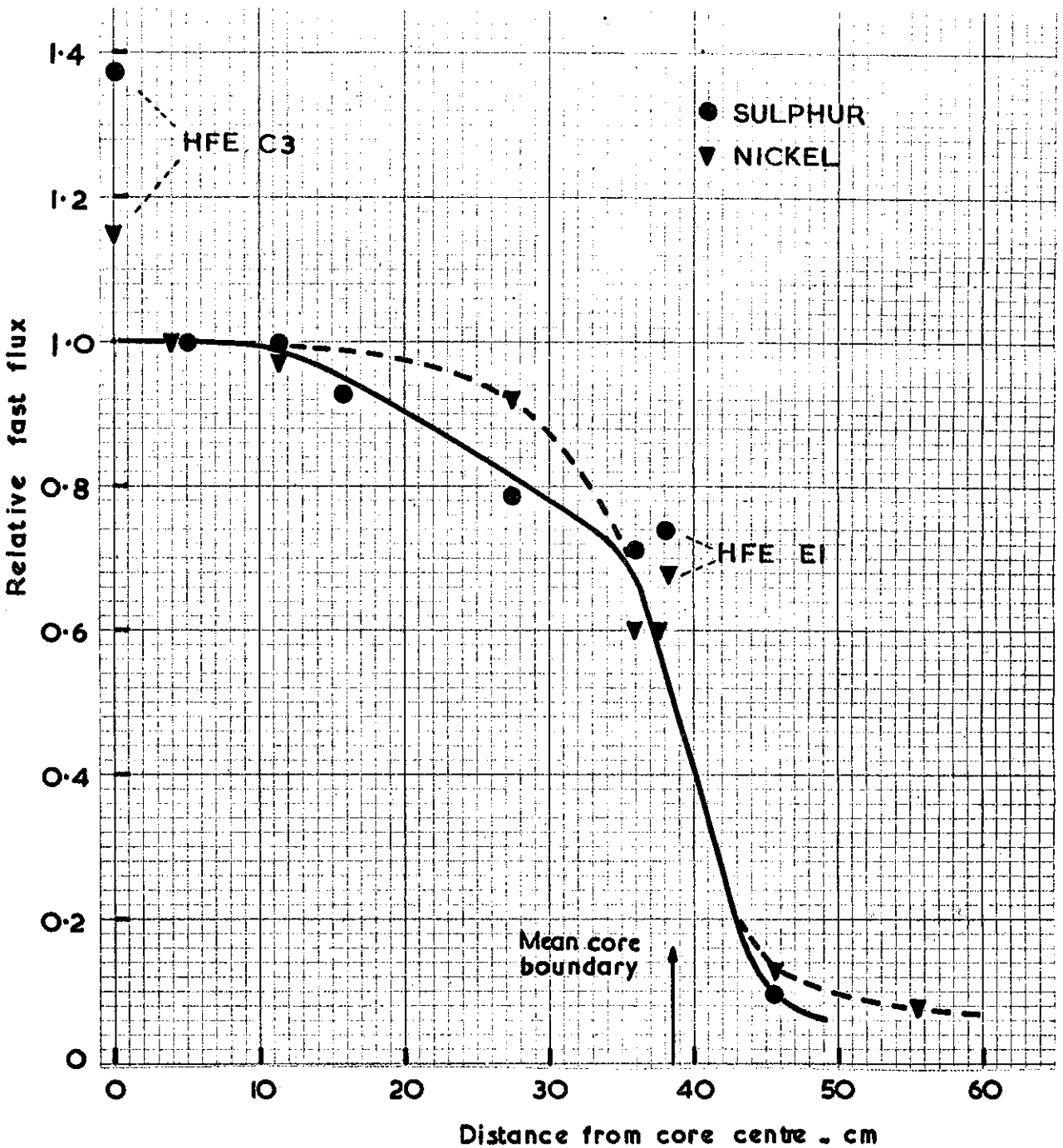

FIGURE 7 RADIAL VARIATION OF FAST NEUTRON FLUX